Tailoring the Ionic Association and Microstructure of Ionomers with Various Metal Salts

Yan Gao, Namita Roy Choudhury, Naba K. Dutta

Ian Wark Research Institute, University of South Australia, Mawson Lakes Campus, Mawson Lakes, Adelaide, South Australia 5095, Australia

Received 24 April 2010; accepted 8 July 2011
DOI 10.1002/app.35214
Published online in Wiley Online Library (wileyonlinelibrary.com).

ABSTRACT: In this work, we investigated the effects of metal stearate salts on the structure, morphology, and properties of poly(ethylene–acrylic acid) neutralized by zinc salts (PI). The samples were characterized in detail with spectroscopic [Fourier transform infrared (FTIR) spectroscopy], microscopic (hot-stage optical microscopy), thermal [thermogravimetric analysis, modulated differential scanning calorimetry, and dynamic mechanical analysis], mechanical, and scattering (small-angle neutron scattering and small-angle X-ray scattering) techniques. The melt rheological properties of the samples were also investigated. The structure of the ionic domains was determined by the type of cations and the salt proportion (FTIR). The predominant interaction was found to exist between the metal stearate and the ionic group. Na^+ cation exhibited a unique behavior, whereas Zn^{2+} showed a coordinated structure and, hence, properties. The ionic groups in the Na and Zn stearate systems existed as multiplets and clusters, but multiplets were the main structure in the Al salt system. The salts acted as plasticizers above their melting points (mp's) but as fillers below their mp's. The melt flow properties of PI were significantly affected by the metal cation and salt proportion and were improved greatly by the introduction of the salts. © 2012 Wiley Periodicals, Inc. J Appl Polym Sci 000: 000–000, 2012

Key words: ionomers; mechanical properties; rheology; thermal properties

INTRODUCTION

Ionic associations present in ionomers act as physical crosslinks; this leads to many of the characteristics of a chemically crosslinked polymer. Specifically, significant increases in the melt viscosity, rubbery modulus, and glass-transition temperature (T_g) are observed because of the presence of these ionic associations.[1–8] Such associations make it possible to produce ionic thermoplastic elastomers, whereas the weakening of the associations at elevated temperatures permits melt processing, but the long lifetimes of the associations at room temperature yield crosslinked, polymer-like behavior. Also, the presence of ionic groups makes the flow behavior complex and significantly increases the relaxation time of polymers. The magnitude of the increase in the relaxation time depends on the type of ion and the polymer backbone, as well as on temperature.[9,10] However, being nonpermanent crosslinks, they can be reversibly disrupted by the application of heat, solvent, stress, or a combination thereof. The ionic associations are, thus, in a dynamic equilibrium condition. Cooper[11] reported that these associations might exist to very high temperatures, even when the interchange of ionic groups (with stress relaxation and promotion of melt flow) was rapid.

The strategy of mixing ethylene ionomers with different metal cations offers some technological advantages because of cation exchange; however, many properties, such as strength, stiffness, and moisture absorption, can also be tailored according to the requirements with plasticizers. Many plasticizers, such as ionic or nonionic plasticizers, have been investigated to assist melt flow.[12–20] The complexity of the flow behavior of ionomers increases with the type of ionic moiety, degree of neutralization, size, and so on. The persistence of strong ionic association even at an elevated processing temperature thus mandates a method that can weaken the ionic interaction. Through the choice of a suitable additive and the cation borne by it, it is possible to obtain ionomers with excellent mechanical properties and sufficiently low melt viscosities. This can be achieved by the addition of a polar ingredient that can plasticize the ionic domains at elevated temperature, only without any detrimental effect on the room-temperature mechanical properties. A variety of such unique ionic plasticizers were described by Makowski et al.[21] In particular, an attractive combination was

Additional Supporting Information may be found in the online version of this article.

Correspondence to: Y. Gao (gaoyan03@yahoo.com) or N. R. Choudhury (namita.choudhury@unisa.edu.au).

TABLE I
Identification of the Samples and Their Thermal and Viscoelastic Properties

Sample	Molar ratio of metal stearate to acrylic acid (mol %)	TGA		DMA	
		T_{max}* (°C)	Weight loss at 420°C (%)	E' −150°C (MPa)	T_i from tan δ (°C)
PI	—	471.4	5.84	4238.2	32.0
PI–NaST-1	5	476.7	6.20	4551.7	37.9
PI–NaST-2	13	477.5	9.08	4418.7	37.9
PI–NaST-3	27	476.7	12.55	4466.2	36.5
PI–ZnST-1	5	476.0	7.11	4399.7	33.9
PI–ZnST-2	13	476.7	8.91	4618.2	33.4
PI–ZnST-3	27	477.5	12.53	4456.7	32.2
PI–AlST-1	5	475.2	6.13	4447.2	36.9
PI–AlST-2	13	477.5	9.23	4485.2	30.4
PI–AlST-3	27	477.5	12.19	4494.7	32.6

* T_{max} = maximum decomposition temperature; E' = Storage modulus

found to be zinc stearate (ZnST) with zinc salt of sulfonated ethylene–propylene–diene monomer. ZnST is known to behave as an ionic plasticizer above its melting point (mp) but as filler at room temperature. Depending on their compatibility, the thermal, mechanical, and relaxation behaviors can vary widely. Therefore, the variation of the transition parameters and different relaxations can be related to the degree of microphase separation, and the change in the size and shape of the cluster due to the addition of a polar additive. In this work, the modification of the ionic association and the microstructure of ethylene ionomer were examined with various metal stearates. Various mechanical, structural and morphological aspects and, in particular, flow behavior were studied in depth to understand the role of such additives.

Various metal stearates, which could dissociate/weaken the ionic interactions and also disrupt the hydrogen bond, were used to ease melt processing. Although a nonionic plasticizer can plasticize both the ionic phase and the nonionic matrix, a polar one can selectively plasticize the ionic domain through associations with the ionic groups at processing temperatures and, thus, assist melt flow. The polar plasticizer can dissociate, therefore, the ionic groups at the service temperature and allow the ionic associations to reform and serve as physical crosslinks. The aims of this work were to tailor the ionic interaction and microstructure with alkaline and transition-metal stearates and to establish their influences on the ionic aggregation, hydrogen bonding, and various other properties, including the melt rheological behavior of the ionomer. The ionomer, poly(ethylene–acrylic acid) neutralized by zinc salts (PI), was used in conjunction with various metal stearates, including sodium stearate (NaST), ZnST, and aluminum stearate (AlST), to vary the level of ionic interaction and, hence, modify the properties. The ideal salt would provide the right melt rheology during processing with enhanced physical properties.

EXPERIMENTAL AND CHARACTERIZATION

Materials

The commercially available ionomer, PI (Iotek 4200), was received from Kemcor Australia. Iotek 4200 was manufactured by Exxon-Mobil with a melt flow index of 3 g/10 min, density (d) = 946 kg/m^3. It contained 11 wt % acrylic acid segments, of which 14 mol % was neutralized by zinc salt. The metal salts used to plasticize PI were NaST (AJAX Chemicals, Ltd., Australia), ZnST, and AlST (CSR Chemicals Pty., Ltd., Australia).

Sample preparation

PI was mixed with various stearate salts in different proportions (Table I) using a Brabender plasticorder at 180°C at a rotor speed of 60 rpm. PI was first melted in the mixer, and then, the metal salts were added. Mixing was done for 3 min. The mixture was then compression-molded to make a sheet at 150°C under a pressure of 31 MPa. The sample was then cooled to room temperature under the same pressure. The samples with metal stearate systems were transparent; this indicated that the stearates remained soluble in the system. The samples were left for 24 h before testing.

Characterization

Photoacoustic Fourier transform infrared (PA-FTIR) spectroscopy was used for the structural analysis of the ionomers. A Nicolet Magna spectrometer (model 750) equipped with an MTEC (model 300) photoacoustic cell (Ames, Iowa) was used. Carbon black was used as the reference. The purge gas used was high-purity helium at a flow rate 10 cc/s.

Thermogravimetric analysis (TGA) of the samples was performed with TA 2950 thermal analyzer (TA Instruments, New Castle, DE) under a nitrogen atmosphere. The samples were heated from 30 to 600°C at a heating rate of 10°C/min. The onset of

degradation, the weight loss due to different ingredients, and the residue remaining were evaluated.

Modulated differential scanning calorimetry (MDSC) was conducted with a DSC 2920 (TA Instruments) to analyze the melting/crystallization behaviors of the samples. The purge gas used was helium at a flow rate of 50 mL/min. The sample (~ 5 mg) was first heated from 30 to 120°C at 20°C/min in DSC mode, then cooled to 30°C at 0.5, 2, and 5°C/min cooling rates, and finally heated again from 30 to 120°C at a 2°C heating rate with an amplitude of modulation of ±0.2°C and a period of 40 s in MDSC mode. The heat flow (HF) associated with the transitions in the materials as a function of time and temperature was measured.

The dynamic mechanical properties of the samples were measured with a DMA 2980 instrument (TA Instruments). The sample size used was 15 × 2 × 0.5 mm^3. The module dynamic mechanical analysis (DMA) multifrequency tension mode was used with a static force of 1 N and a frequency 1 Hz. The sample was heated from −150 to 100°C at 3°C/min heating rate. Thermal analysis of each sample was done in duplicate. The scatter between the experimental results was ±2%.

Hot-stage optical microscopy (HSOM) was used to measure the phase transitions and crystallization kinetics of the polymers. Microtomed samples (40 μm thick) were placed on a microscope slide, and a cover glass was fixed over it. The slide was then heated at a heating rate of 2°C/min to 120°C, held for 4 min, then cooled to different temperatures at a cooling rate of 2°C/min, and finally cooled to 30°C at 0.5°C/min. The images were recorded on video with representative images captured during cooling with the IP Lab image analysis program (Scanalytics IPLab for Windows, Buckinghamshire, UK), and the temperature was recorded at the time of capture.

Small-angle X-ray scattering (SAXS) data was obtained at room temperature with compression-molded films with a Bruker (Östliche Rheinbrückenstr, Germany) SAXS instrument. The sample-to-detector distance used was 62.7 cm. The X-ray source employed was from Cu Kα radiation with a wavelength of 1.54 Å. The scan range of 2θ was from 0.15 to 5°.

Small-angle neutron scattering (SANS) measurements were carried out at the national SANS facility at the Australian Nuclear Science and Technology Organisation (Lucas Height, New South Wales). Samples 1 mm thick were placed in an automatic holder and exposed to the neutron beam for a total of four times for 1 h. Data were collected on the 10-m SANS instrument. The neutron's wavelength was 3 Å. The scattered neutrons were collected on a two-dimensional position sensitive detector. The sample-to-detector distance used was 5000 mm. The q range used was 0.012–0.14 $Å^{-1}$. The scattered intensity data were placed on an absolute scale by their comparison with scattered intensity from a standard sample (porous silica) collected under identical experimental conditions.

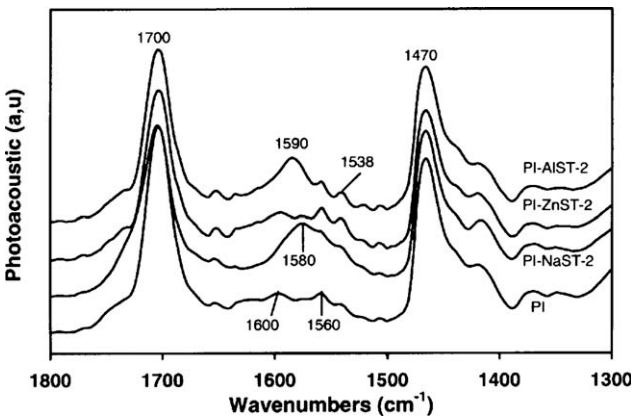

Figure 1 FTIR spectra of PI and PI–MST-2 at 13 mol %.

The rheological properties of the samples were investigated with an AR 1000N instrument (TA Instruments) under oscillation mode. Isothermal measurements were taken in the temperature range 115–155°C over the frequency range 0.1–50 Hz. The sample was placed between the parallel plates and heated to the desired temperature under a nitrogen atmosphere. The quantities measured were the in-phase and out-of-phase components of the shear stress, from which the shear storage modulus (G') and loss modulus (G'') were calculated.

The relationship between the force and fractional deformation was measured according to the ASTM D 882-97 specification. The stress–strain behavior of the materials was also studied.

RESULTS AND DISCUSSION

Structural investigation by PA-FTIR spectroscopy

The effects of various amounts of NaST, ZnST, and AlST on the ionomer's structure were investigated with PA-FTIR spectroscopy. Figure 1 shows the superimposed Fourier transform infrared (FTIR) spectra of the ionomer with various metal stearates (MSt) at 13 mol %. All of the spectra were corrected with linear baseline correction for peak intensity comparison. The main differences in the spectra of the original ionomer and the samples prepared by mixture with different salts were observed in the region 1300–1800 cm^{-1} (Fig. 1). The intense band at 1700 cm^{-1} was ascribed to the C=O stretching mode peak from the unneutralized acid or hydrogen bonded —COOH group. No shift was observed for this peak with the type of salt used. However, its intensity decreased and became broader with increasing proportions of stearate present. This observation

indicated that the metal salt also acted as a hydrogen-bond disruptor, which lowered the extent of such bonding. The effect of different salts on the local structure of the ionomer is clearly revealed in Figure 1. For the PI–ZnST systems, a comparison of the spectra in the range 1530–1650 cm^{-1} clearly revealed that because of the presence of the same cation (zinc), the spectra of the ionomer and PI–ZnST-2 displayed similar doublet peaks at 1560 and 1600 cm^{-1}, respectively; however, the peak intensities marginally increased with the addition of ZnST. Thus, the local structures of PI and PI–ZnST-2 were much the same at such low salt proportions and also provided strong evidence that ZnST appeared in the ionic region, not in the polymer matrix. PI–NaST-2, on the other hand, showed a broad peak centered at 1580 cm^{-1} with a hint of two satellite peaks, and PI–AlST-2 showed a narrow peak at about 1590 cm^{-1} with two satellite peaks. These results demonstrate that the local structure of the ionomer was changed to some extent with the addition of Na and Al salts. In addition, the structure also depended on the size and valence of the metal cations. The major broad peaks in the spectra of PI–NaST-2 and PI–AlST-2 occurred at different wave numbers; this indicated the different strengths of the ionic group interactions.

In the samples with various levels of NaST (Supporting Information, Fig. A), no band for the free acid group was detected at 1750 cm^{-1}. A clear difference was noticed between the samples in the region 1500–1660 cm^{-1} that reflected one broad peak flanked by two shoulders. The main peak did not shift with the proportion of NaST; however, the shoulders at 1560 and 1538 cm^{-1} became more prominent and shifted to lower wave numbers. The peaks in this range were ascribed to the local structures of ionic groups from multiplets (low wave numbers) to clusters (high wave numbers). These two bands were related to the asymmetric stretching vibration of the carboxylate groups in the ionic multiplets and in the ionic clusters, respectively,[22–25] and as the proportion of metal salt in the multiplets increased, the local structure became more complex.

In the samples with various levels of ZnST (Supporting Information, Fig. B), two peaks were observed in the region 1500–1660 cm^{-1}. In PI–ZnST-1 systems, the peak at 1600 cm^{-1} was due to the stretching of the carboxyl ($-COO^-$) group and indicated that the local structure of Zn salt was mainly zinc acid salt. The peak at 1560 cm^{-1} was relatively smaller than the peak at 1600 cm^{-1}. ZnST also showed a strong band at 1538 cm^{-1} due to asymmetric carboxylate stretching of zinc carboxylate (vibration of tetracoordinated zinc carboxylate and hexacoordinated zinc carboxylate multiplets).[24] In PI–ZnST-2, the relative intensity of the peaks at 1560 and 1538 cm^{-1} increased relative to the peak at 1600 cm^{-1}; this indicated increasing multiplet content. In PI–ZnST-3, the peak at 1538 cm^{-1} became the main peak with a shoulder at 1560 cm^{-1}, whereas the peak at 1600 cm^{-1} decreased; this indicated the presence of plasticizer within the ionic domain. These results indicate that the ionomer at low ZnST level had the same local structure as that of PI and, at higher levels, (PI–ZnST-3) remained in tetracoordinated zinc carboxylate and hexacoordinated zinc carboxylate multiplet forms.

The AlST system showed one peak at 1590 cm^{-1} with two shoulders at lower wave numbers (Fig. 1). The peak shifted to higher wave numbers with increasing AlST level (the FTIR absorption spectrum of AlST is shown in the Supporting Information, Fig. C, for reference). Currently, there are no reports on how trivalent metal cations influence the structure of ionomers. In general, in the presence of Al^{3+} salts, the dominant ionic structure was multiplet with some clusters, so the peak wave number shifted. At the same time, because of the existence of other kinds of aggregation, either peak broadening occurred. The structure of the ionic groups in the ionomer became complex with higher valence of metal cations and salt level. At higher stearate levels, the system exhibited phase-separation behavior with the metal salt resident in the ionic domain.

Thermal stability

TGA was used to evaluate the thermal stability and the decomposition pattern of the ionomer with various metal salts. After the preparation of the samples, they were kept in desiccators to prevent moisture absorption before the TGA measurements. Thermogravimetric–differential thermogravimetric curves of PI were reported in our earlier communication.[26(a)] Table I lists the maximum decomposition temperature of all of the samples. The weight loss–temperature curves (Supporting Information, Fig. D) showed a major peak at 471.4°C (PI) due to the decomposition of the ionomer. However, a two-step weight loss pattern was observed in the NaST systems: the first one due to the decomposition of metal stearate (200–400°C) followed by the subsequent decomposition of the ionomer (>400°C). The initial weight loss ranges were from 5 to 20% in the PI–NaST systems, related to the uncomplexed organic acid.[26(b)] The thermogravimetric curves of the samples with NaST shifted marginally to higher temperatures ($\sim$ 5°C) compared to PI; this indicated that NaST did not affect the thermal stability of PI. The residue followed the order: PI–NaST-3 > PI–NaST-2 > PI–NaST-1 > PI. The ZnST and AlST systems showed a similar trend. When we compared the samples with various salt levels, it was clear that the maximum

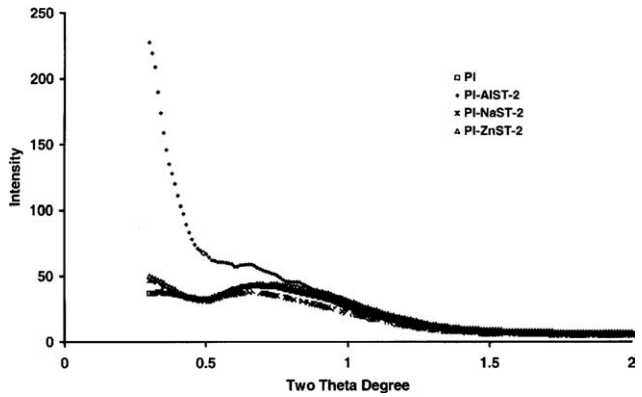

Figure 2 SAXS profiles of PI and PI–MST-2 at 13 mol %.

decomposition temperature changed marginally and indicated that the thermal stability of the ionomer remained invariant with the addition of various metal salts.

Microstructure and morphology

The ionic microstructure of the representative samples were determined with SAXS and SANS. Figure 2 shows the SAXS profiles of PI with various metal salts at 13 mol %. A peak was observed in the scattering pattern for most samples in a scattering angle range of 0.5–1°. The ionomer curve showed one peak (0.69°, 128 Å) and an upturn at a very low angle. Although this peak was the evidence of microphase separation in the ionomer, there is no model that can describe the size, shape, and distribution of the ionic domain. The PI–NaST-2 curve showed that the cluster peak shifted to a lower angle (0.65°, 136 Å) compared to PI. The increase of the cluster size in low-angle scattering also suggested that the local structure of the ionic domains was modified by the addition of NaST and revealed the presence of Na cations in the ionomer cluster. This process reorganized the domain microstructure and allowed the incorporation of the metal salt; this, thereby, increased the volume fraction of the cluster present in the sample. In addition, it increased the size and the electron density difference between the matrix and the cluster. The intensity of the upturn for PI–NaST-2 was also higher than that of PI; this indicated the presence of the ions in the ionic domains. The presence of those two features represented two-distinct environments of the ions, that is, clusters and multiplets. In particular, the upturn (or low-angle scattering) originated because of the inhomogeneous distribution of isolated ionic groups. The SAXS curve of PI–ZnST-2 demonstrated that the cluster peak (ionic domain) did not shift but became broader compared to PI. This observation indicated that the cluster size of the ionomer was independent of the ZnST proportion, but the local structure of the ionomer became more complex with increasing salt content. The result of the addition of PI–AlST-2 was obviously different from other samples. The ionic peak intensity increased and shifted to a lower scattering vector (indicating a larger size). A very high upturn intensity appeared, and the cluster peak occurred at 0.66° (134 Å), which was lower than that of PI. The PI–AlST-2 results demonstrated that the ionic groups mainly existed as multiplets rather than clusters. The appearance of the small cluster peak was due to Zn salt from the ionomer. The shift of the peak to a lower angle suggested that some Al cations also resided in the clusters. When we compared the samples examined, it was clear that monovalent and divalent salts existed in the clusters and that multiplets in the ionomer and the quantity of the clusters and multiplets depended on the salt levels, but trivalent cations gave rise to multiplets, which acted as ionic association disruptors. Various metal salts in the ionic phase changed the electron density contrast between the matrix and clusters and reduced the volume fraction of the cluster in the ionomer, which resulted in reduced ionic peak intensity.

The microstructure of the ionomer was also investigated as a function of metal cation (Na and Al) with SANS. Figure 3 exhibits the SANS profiles of PI, PI–NaST-2, and PI–AlST-2. A distinct upturn was observed in all of the samples, followed by a broad peak, which was associated with the ionic region. The intensity of the upturn was higher for the ionomer with the salts than that for neat PI. This trend indicated that the volume fraction of separated ion-rich aggregate increased because of the addition of stearate salts.[27] The maximum scattering intensity was observed corresponding to an average spacing (calculated with $d = 2\pi/q$). The upturn appeared at $q = 0.11$ nm^{-1} ($d = 57$ nm) for PI and $q = 0.13$ nm^{-1} ($d = 49$ nm) for PI–NaST-2 and PI–AlST-2. The nature of the small peak for PI–NaST-2 and PI–AlST-2

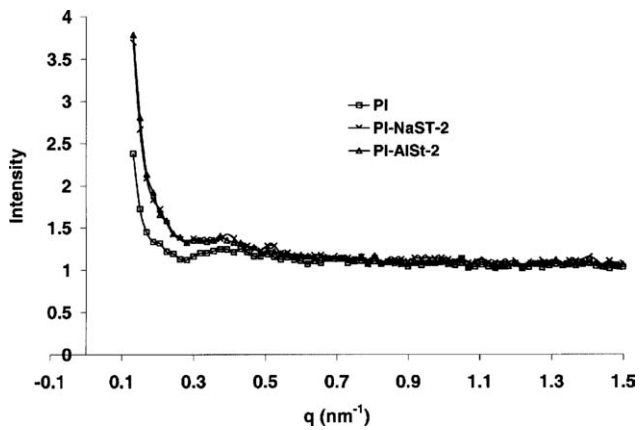

Figure 3 SANS profiles of PI, PI–NaST-2, and PI–Al ST-2.

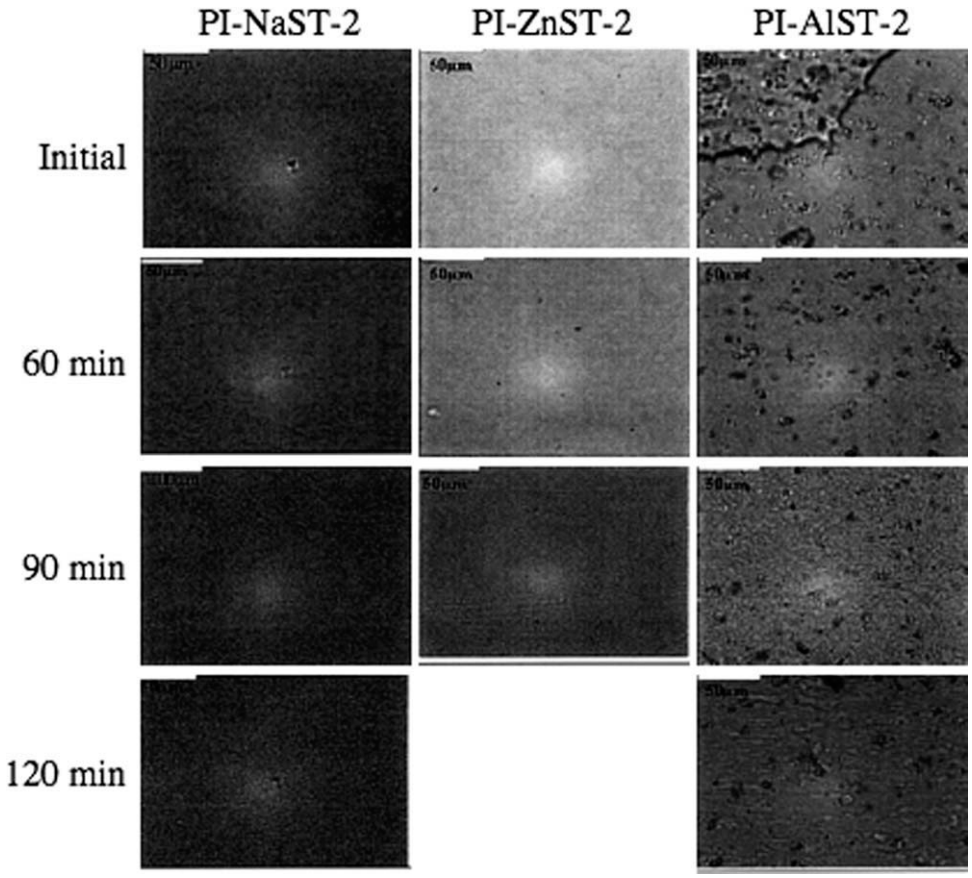

Figure 4 Polarized optical microscopy pictures of PI–NaST-2, PI–ZnST-2, and PI–AlST-2 after various cooling times from the melt (the scale bar at the top left corner is 50 μm.).

was similar. The position of the peaks essentially merged with the small angle upturn.

HSOM was performed to visualize the effect of metal salts on the melt crystallization behavior of the ionomers. The micrographs of PI after crystallization at various times (0–120 min) were shown and discussed elsewhere.[28] In this work, only the polarized optical microscopic images of PI–NaST-2, PI–ZnST-2, and PI–AlST-2 are shown in Figure 4. The images of PI–NaST-2 show that PI–NaST-2 was in the melt form at 100°C (initial), with some crystals at 87.5°C (after 60 min) and with more crystals at 85.0°C (after 90 min). At 58.0°C (after 120 min), a homogeneous spread of small finer crystals was clearly observed. In PI–ZnST-2, the crystallization process showed a similar trend as that in PI–NaST-2. PI–AlST-2 was in the melt state at 100°C, and the existence of small crystals was obvious because of the presence of AlST. The crystals grew with decreasing temperature. It was noted that an extent of phase separation existed in these four images. The dark areas represented AlST, and the light area was the ionomer matrix. Solid AlST acted as a nucleating agent for the crystallization process during cooling. The crystallization of the polyethylene (PE) phase started in the presence of AlST. The crystallization process of PI–AlST-2 was somewhat different from that of the other samples. It showed a droplet matrix structure with the ionomer as the continuous phase and AlST as isolated domains in the matrix. Less defined crystals of the ionomer due to the ionic groups and the metal salt were evident under HSOM. It indicated a lower level of crystallinity, as also confirmed from MDSC (discussed later). The results indicate that the ionic domains restricted the formation of the nonspherulite, which was dependent on the type of metal cations. The images show that fine crystals occupied the complete area at 85°C, and the amorphous regions could exist in the interunspherulitic area of PI, PI–NaST-2, and PI–ZnST-2. At all experimental temperatures, PI–AlST-2 showed the presence of smaller crystals but a more coarse morphology than the rest. It appeared that the melt went through homogenization and refinement and crystallized under HSOM; this led to a more even distribution of the stearate droplet in the matrix.

Differential scanning calorimetry (DSC) was also used to determine the influence of metal stearate on the melting and crystallization behaviors of the ionomers. PI showed the order–disorder transition of ionic cluster at 53.2°C and the melting of PE at 95°C.[28] Table II lists these two transition

TABLE II
Cluster Transition and PE Melting Temperature from DSC

Sample	T_i (°C)	PE melting temperature (°C)	Sample	T_i (°C)	PE melting temperature (°C)
PI	53.2	96.2	PI–ZnST-2	56.2	95.5
PI–NaST-1	52.1	97.1	PI–ZnST-3	56.7	94.8
PI–NaST-2	51.6	97.0	PI–AlST-1	53.8	96.9
PI–NaST-3	51.4	96.0	PI–AlST-2	55.9	95.6
PI–ZnST-1	54.5	95.9	PI–AlST-3	53.0	96.8

temperatures for all of the experimental samples. The results show that the PE melting temperature did not change with the addition of metal stearate; this indicated that the metal salts did not plasticize the polymer matrix. This result was in line with the DMA observation (discussed later). The cluster transition temperature was affected marginally by various metal salts and their concentrations.

The samples were also examined with MDSC. The total HF, reversing heat flow (RHF), and nonreversing heat flow (NHF) of the samples and the crystallinity obtained from the MDSC results at a 0.5°C/min cooling rate are listed in Table III. The MDSC curves of PI are reported in our earlier communication.[28] The MDSC curves of PI–NaST samples were similar to those of PI; this indicated that the addition of NaST did not affect the morphology of the PE crystals (Supporting Information, Fig. E). However, Table III shows that the reversing and nonreversing components did change. RHF increased, whereas NHF decreased with increasing NaST proportion. This result demonstrates that the presence of NaST reduced the melt entanglement density and increased the number of multiplets and ionic domains. However, the total HF values due to melting of the PE phase of the ionomer in these samples were similar. Metal stearate salts could contribute two different effects: (1) metal stearate could form small ion-rich zones or multiplets and increase their numbers and change the crosslink density to restrict PE crystal formation, and (2) stearate groups could reside in the clusters or outside the remaining microphase-separated region and act as fillers, and/or the stearate groups could remain miscible with PE phase, so some crystals were formed, including PE chains and stearate groups, which resulted in a more homogeneous system. Duvdevani et al.[29] and Jackson et al.[30] made similar observations and reported that ZnST formed small crystallites that acted as fillers. These crystallites were presumed to interact with the ionic groups to give good adhesion between the filler and polymer.

In ZnST samples, RHF, NHF, and total HF were similar. This observation indicated that the morphology of the PE crystal was independent of the ZnST content. PI–AlST-1 and PI–AlST-2 showed a similar reversing component, but a higher value was observed for PI–AlST-3 compared to PI. The NHF and total HF decreased with increasing salt proportion. The crystallinity of the PE phase decreased as well. This was because Al^{3+} needed three $-COO^-$ groups for interaction. The size of ionic domains was bigger and looser with more free volume than that formed from monovalent and divalent metal cations. The shoulder for folded chains shifted to lower temperatures with increasing content of NaST and AlST; this indicated that the morphology and the microstructure of the ionic domains in the ionomer were different with various amounts of metal salts. The results for the divalent ZnST systems clearly show a difference between the monovalent and trivalent salts. The shoulder in NHF and total HF only appeared at a 0.5°C/min cooling rate, indicating that the addition of ZnST reduced the formation of folded chains. The ionic transition peak

TABLE III
Effect of Various Metal Salts on the Melting Behavior of PI from MDSC

	RHF		NHF		HF		
Sample	J/g	Temperature (°C)	J/g	Temperature (°C)	J/g	Temperature (°C)	Crystallinity (%)
PI	15.3	90.6	45.4	94.9	60.7	94.4	20.9
PI–NaST-1	19.5	92.6	40.1	95.2	59.6	94.6	20.6
PI–NaST-2	25.0	92.9	34.9	95.9	60.0	95.2	20.7
PI–NaST-3	22.1	90.7	33.5	95.1	55.5	94.8	19.2
PI–ZnST-1	13.2	90.0	45.1	94.8	58.3	94.4	20.1
PI–ZnST-2	12.8	90.4	43.2	94.0	56.0	93.5	19.3
PI–ZnST-3	12.5	89.5	40.3	93.8	52.8	93.1	18.2
PI–AlST-1	14.5	92.3	43.6	95.3	58.1	94.8	20.0
PI–AlST-2	13.1	91.2	39.2	94.9	52.2	94.1	18.0
PI–AlST-3	19.3	91.8	34.5	96.0	53.8	95.4	18.5

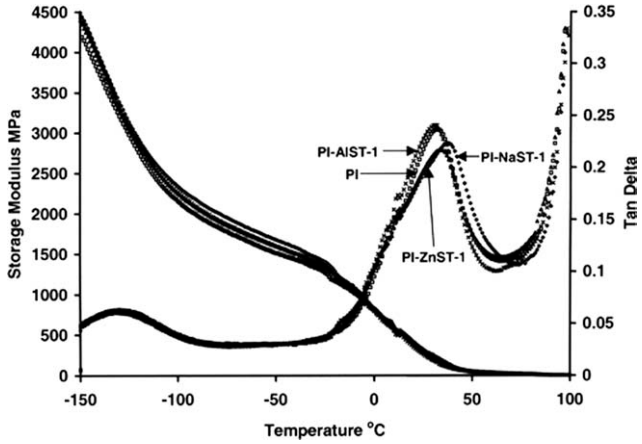

Figure 5 Plots of E' and tan δ as a function of temperature for PI with and without metal salts.

did not appear in the MDSC run. This was because formation of clusters was time-dependent.[28] In all the systems, the crystallinity dropped with the addition of various metal salts in different proportions (Table III).

Dynamic mechanical properties

The dynamic mechanical properties of the ionomer were studied as a function of various metal stearates to understand the viscoelastic behavior and to make a structure–property correlation. The E' and tan δ values of the ionomer are shown in Figure 5 as a function of various metal salts at 5 mol % PI–MST-1 (where M is metal). The values of E' and the ionic transition temperature (T_i) of the ionic groups are listed in Table I. E' in all cases decreased with increasing temperature and was close to zero at 100°C because of the onset of the melt flow of the samples. A significant drop in E' was also observed in all samples below −100°C followed by a plateau in the range of −100 to −40°C, which was related to T_g of the PE phase. In all the samples, T_g of PE did not change; this indicated that the metal stearate salts did not affect the amorphous part of PE. The second dramatic drop of E' for all samples was observed from −25 to 50°C, corresponding to the cluster transition. E' of the ionomer was improved with the addition of the salts but changed marginally between the samples with metal salts (Table I). E' above 0°C did not show a difference between the samples; this indicated that the metal salts acted as fillers in the cluster below the cluster transition. T_g of PE and the cluster transition temperatures found from the tan δ curves were −130 and 32°C, respectively.[26] Table I shows that the cluster transition temperature (from tan δ) did not change very much with the addition of ZnST and AlST (with the exception of PI–AlST-1). The tan δ curves (Fig. 5) showed a sharp upturn after 70°C, which was related to the melt flow of PE phase, which was not affected by the salt proportions but by the metal cations. Similar behavior of metal stearates was also reported earlier, where they acted as ionic plasticizers,[14,17] which selectively plasticized the ionic regions as a result of their preferential segregation in the ionic template. Such salts show temperature-dependent functions. Above its mp, the salt behaved as a melt flow promoter, but it acted as a filler at ambient temperature.

Melt rheology

The melt rheological properties of the ionomer and its compounds were measured over a range of frequency and temperature. The dynamic G' is shown in Figure 6(a) as a function of frequency at 125°C for

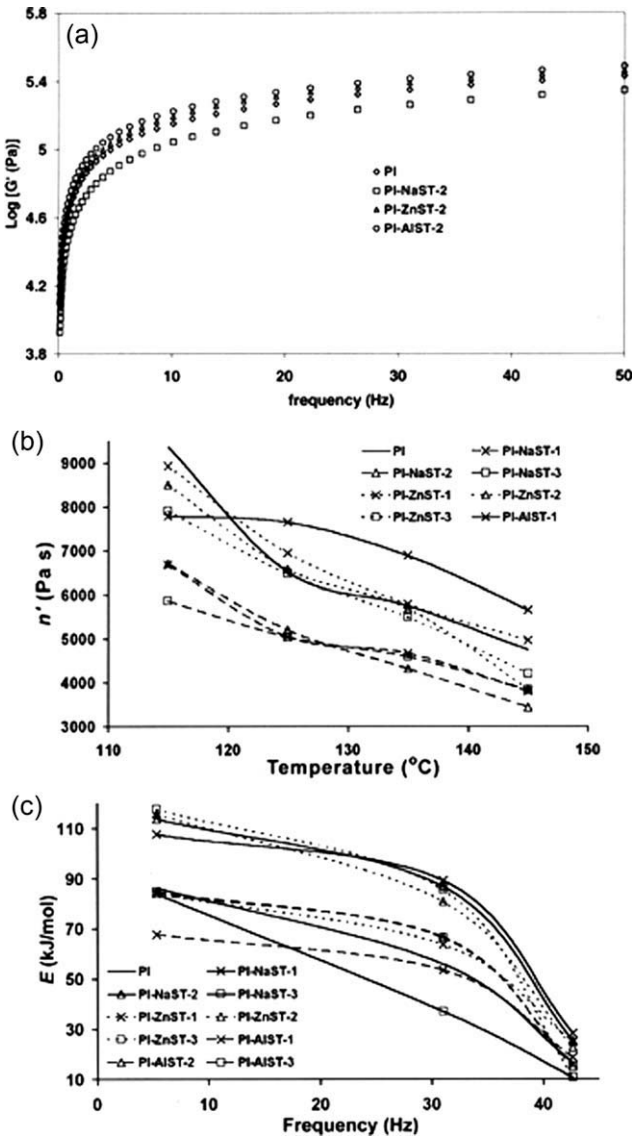

Figure 6 (a) G' as a function of frequency curves for various PI–metal stearate systems at 125°C. (b) Plot of viscosity (η*) as a function of temperature for PI with various proportions of metal salts at 1.089 Hz. (c) E of the melt flow as a function of frequency for various systems.

PI, PI–NaST-2, PI–ZnST-2, and PI–AlST-2 systems. The G' and G'' (not shown) values of all of the samples increased with frequency and followed the order: PI–AlST-2 > PI–ZnST-2≈PI > PI–NaST-2. This result shows that at 125°C, the melt behavior of PI was affected by the addition of metal salt. The addition of NaST reduced the shear modulus of the ionomer, whereas the addition of AlST increased the shear modulus, but the introduction of ZnST did not change the flow behavior of PI. G' and G'' decreased with increasing temperature in all of the samples. It must be noted that each stearate salt melted at a different temperature. NaST melted at 110°C. Therefore, during rheological measurement at 125°C, it acted as a flow promoter or plasticizer. On the other hand, ZnST and AlST melted at higher temperatures (130 and 150°C, respectively), so they remained as fillers. The samples showed similar behaviors at 115 and 125°C. At 145°C, the G' and G'' curves of all the samples were lower than those of PI; this indicated that the melt flow of the ionomer was promoted by the addition of metal salts. Metal salts acted as plasticizers, disrupting the ionic association. Thus, all of the metal salts below the mp acted as fillers, but above the mp, they acted as plasticizers; this has also been reported by other investigators.[29]

The effects of the type and level of metal salts on the viscosity of the ionomer are shown in Figure 6(b) as a function of temperature. As expected, the viscosity of all of the samples decreased with increasing temperature. In most cases, the drop in viscosity was more prominent up to 130°C except PI–AlST-1, as these metal salts (NaST/ZnST) acted as plasticizers at this temperature. The salts reduced the viscosity of the ionomer either by solvation or by a shear-induced exchange reaction between the salts and the carboxylate group.[31] The viscosity drop of PI–AlST-1 was prominent at higher temperatures because of the higher mp of AlST. In the NaST system, the viscosity changed marginally with the salt level [Fig. 6(b)] but was lower than that of PI; this indicated that NaST acted as an efficient flow promoter. In ZnST systems, the viscosity decreased with increasing salt content at low temperature, independent of the salt content at high temperature. The decrease in the viscosity followed the order $Al^{3+} < Zn^{2+} < Na^{+}$. Nishio et al.[32] reported that the zero-shear viscosity of poly (ethyl methacrylic acid)-EMMA ionomers depended on the kind of metal cations. Xie and Ma[33] observed the same phenomenon in their sulfonated ethylene–propylene–diene monomer ionomers.

For polymer materials, above their softening temperature, the viscosity follows an Arrhenius trend. To compare each material's ability to flow and relate that to plasticization, the activation energy (E) of the melt flow processes at a constant frequency was calculated with an Arrhenius equation: $n' = A \exp(E/RT)$, where n' is the viscosity at a constant frequency, A is a constant, R is the gas constant, and T is the temperature. The plots of activation energy, E of the melt flow as a function of frequency for various systems are shown in Figure 6(c). For all samples, E decreased with increasing frequency, showing shear thinning nature. In the NaST systems, E followed the order PI–NaST-1 ≈ PI–NaST-2 > PI > PI–NaST-3. E thus reflected the ease of flow due to the interaction force between the polymer chains when cooperative motion started. It was clear that NaST acted as a plasticizer; this indicated the reduction of the ionic association with the addition of NaST. An increase in E of the ionomers with the addition of plasticizers was observed by Granick[34] and Xie and Ma.[33] Often the addition of plasticizers to an ionic polymer increases the number of ionic domains but decreases their size, which subsequently increases the number of crosslinks. Thus, E of melt flow increased. E in ZnST and AlST systems showed an increase with increasing salt proportion and changed marginally at higher proportions.

The G' and G'' values as a function of the angular frequency for PI–NaST-1 (Supporting Information, Fig. F) increased with frequency and displayed a linear log–log relationship over the range of experimental temperatures. They decreased with increasing temperature. All of the experimental samples showed similar characteristics to those of PI–NaST-1. We observed that the viscoelastic function for PI–NaST-1 measured at various temperatures and frequencies could be superimposed onto a master curve with time–temperature superposition (TTS). The TTS master plot was constructed on the G' and G'' data with TA Instruments TTS software with a reference curve at 125°C.[35] Figure 7(a) shows the master curves of G' and G'' as a function of frequency for PI–NaST-1. Both G' and G'' obeyed the TTS principle; therefore, the curves at different temperatures were found to superimpose well on a master curve. This observation indicated that PI–NaST-1 was a thermorheologically simple system within the experimental range. The shear modulus curves of each sample at low stearate contents showed excellent superposition, and the curves of both moduli (G' and G'') were superposable by application of the same shift factors; this indicated the materials to be thermorheologically simple at low ion content. However, the master curves failed for the samples with high ion contents (within the experimental range); this indicated thermorheological complexity. The microphase separation in these ionomers affected their dynamic rheological properties.[36,37]

G' and G'' master curves with various ionic contents were also constructed with the Arrhenius shift factor. Figure 7(b) shows the superimposed G' and G''; master curves of the samples with various ZnST

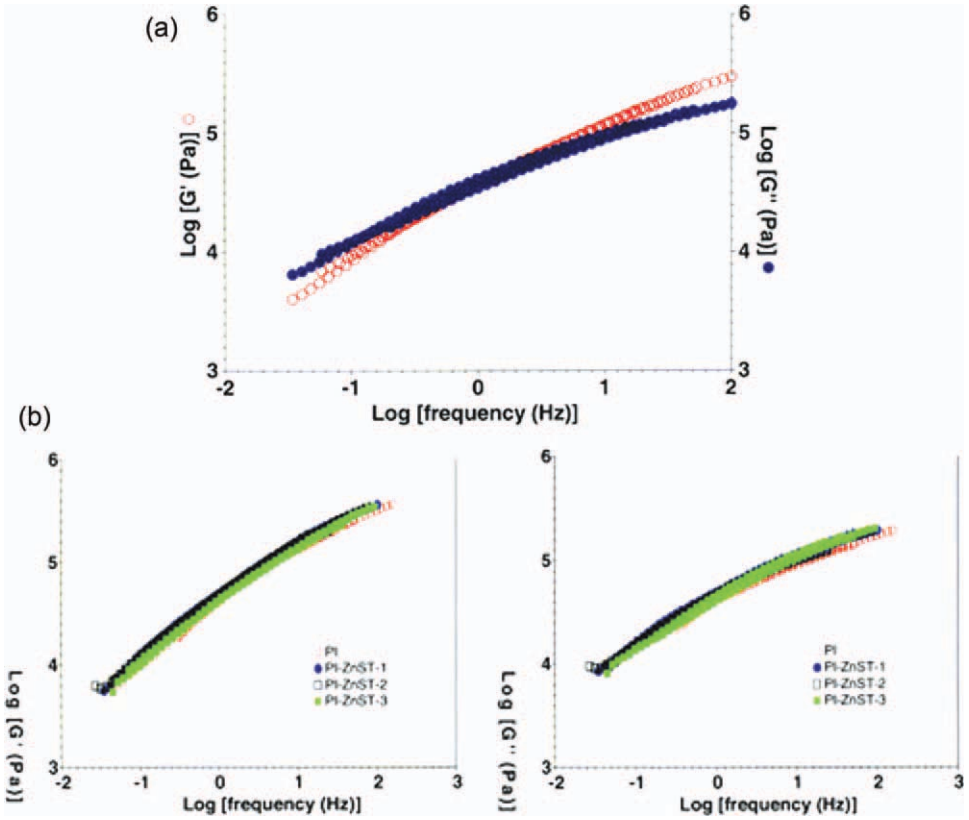

Figure 7 (a) G' and G'' master curves of PI–NaST-1. (b) G' and G'' master curves of PI with various ZnST contents. [Color figure can be viewed in the online issue, which is available at wileyonlinelibrary.com.]

contents. The samples with various ZnST levels showed similar results to those of PI and indicated that the melt flow behaviors were independent of this metal salt. A similar trend was observed by Duvdevani et al.[29] and Jackson et al.[30] However, the G' and G'' master curves for the ZnST and NaST samples showed dependency on the ionic contents. The melt flow behavior of the ionomer did not change with ZnST proportion in our study. The master curves with AlST showed an increase with ionic content and then dropped dramatically at 27 mol % AlST loading.

Differences in the rheological behavior certainly existed [Fig. 6(a)] when different salts were employed. When the ratio of stearate to acrylic acid was 13 mol %, the G' and G'' values of the samples, except PI–AlST-2, were lower than PI. The G' and G'' values of PI–AlST-2 were much higher than PI, which indicated that G' of PI increased at such AlST content. With AlST, an ester interchange reaction could occur where it remained strongly associated with the ionic group or it disrupted the ionic domain due to higher ionic potential; this increased the number of multiplets or crosslinks. The results at 5 mol % show that the PI–AlST-1 master curves were above that of PI–ZnST-1, which were the same with PI, whereas PI–NaST-1 showed the lowest moduli. This indicated that the melt rheology behavior of the ionomer depended on the type of metal salt. NaST primarily acted as a plasticizer at various proportions.

At 27 mol % ion content, TTS curves were obeyed only in the ZnST system. At higher NaST and AlST proportions, the TTS curves failed. This was due to further complexity in the melt flow behavior. Thus, the motion of different kinds of molecular systems in a chain exhibited temperature dependencies. In general, plasticizers increased the rate of relaxation. Thus, in the studied poly(ethylene acrylic acid) ionomer, two relaxation processes were prominent, one of which may have been too rapid or too slow to be apparent in the timescale studied.[38] Plasticizers could change the rate of the PE melting relaxation process sufficiently so that the relaxation processes appeared in the studied timescale. It was clear that the addition of metal salts or so-called polar plasticizers to the ionomers led to a lowering of the microphase separation, which thereby changed the rate of the second relaxation process.

Mechanical properties

The mechanical properties of all of the samples were determined from the stress–strain measurement.

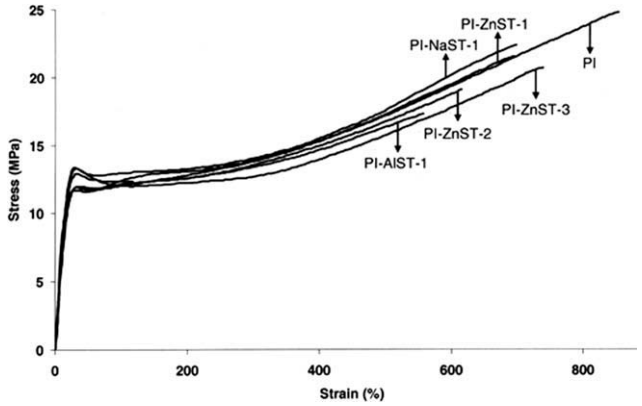

Figure 8 Effect of metal stearates on the stress–strain behavior of PI.

Figure 8 shows the stress–strain curves of the ionomer with various proportions of ZnST, PI–NaST-1, and PI–AlST-1. The typical curve, in all cases, showed a linear relationship between the stress and strain at a very low strain regime followed by a yield point, and finally, strain-hardening behavior was observed before fracture. PI had the lowest yield stress. The yield stress increased with increasing ZnST proportion; this indicated that the addition of salts improved the mechanical properties of the ionomer. It was noteworthy that the elastic properties beyond the low range of stress or strain were deteriorated to some extent by the addition of metal stearate. Thus, the strain at break decreased significantly compared to that of PI; this indicated that the elongation of the specimens after yielding decreased as the ZnST content increased. The ionomer became more brittle with increasing salt content. The stress at break also decreased with increasing salt content. A higher modulus and stiffness in a sample, which is seen in the elastic region, represents a higher stress for similar strain. Such stress can accelerate the ion-hopping process efficiently in the presence of metal stearate and result in a loss of integrity of the ionic domains and, hence, of physical crosslinks. Thus, the breaking strength of the ionomer decreased with the addition of metal stearate. The yield stress values of the samples in NaST and AlST systems were also higher than that of PI but changed marginally with the salt content. The elongation at break decreased in the NaST/AlST system. The yield stress and the elongation at break for different types of salts followed the order $Na^+ > Zn^{2+} > Al^{3+}$. The enhancement in the mechanical properties of the ionomer was more marked in the NaST system. It has been reported that the tensile strength of ionomers was in direct proportion to the ionic potentials of the metal cations.[33] The ionic domains are more dispersed in a high ionic potential system; therefore, the tensile strength of the ionomer is higher.

CONCLUSIONS

The effects of type and level of metal stearate in tailoring the properties and improving the melt flow behavior of ionomers were examined in this work. From the thermal, thermomechanical, rheological, and microscopic results, it was evident that the metal stearate acted as an ionic plasticizer in the melt state. Most of the samples were clear and transparent at room temperature; this indicated the solubility of the stearate in the polymer matrix. The addition of metal stearate resulted in predominant interaction between the metal stearate and the ionic groups rather than between the ionic groups. The organization of the ionic domains was related to the size and charge of the metal cation and the distance between the ion pair. In most cases, Na^+ exhibited unique behavior, whereas Zn^{2+}, due to its partial covalent nature, showed a coordinated structure and, hence, properties.

The morphological studies revealed that the ionic groups in the NaST and ZnST systems existed as both multiplets and clusters, depending on the salt proportion, but multiplets were the main structure with some in ionic domains in the Al system. G' of the ionomer improved with the addition of the salt but changed marginally with the salt content and the type of metal cations. The crystallinity of the ionomer did not change with the addition of the salt. The melt rheology results show that the melt flow properties of the ionomer were improved greatly with the introduction of the salt. NaST showed enhanced flow characteristics and was the most efficient plasticizer among the different salts investigated. The addition of metal salts enhanced the mechanical properties of the ionomer, but the elongation at break was reduced. The metal stearates, thus, mainly affected the characteristics of the ionic domain and acted as fillers below their mp's but as plasticizers above their mp's.

References

1. Lantman, C. W.; MacKnight, W. J.; Lundberg, R. D. In Comprehensive Polymer Science: The Synthesis, Characterization, Reactions & Applications of Polymers Polymer Properties; Allen, G., Bevington, J. C., Booth, C., Price, C., Eds.; Pergamon: United Kingdom, 1989; Vol. 2, p 755.
2. Eisenberg, A.; Kim, J.-S. Introduction to Ionomers; Wiley: New York, 1998.
3. Holliday, L. Ionic Polymers; Applied Science: London, 1975.
4. Varley, R. J.; Shen, S.; van der Zwaag, S. Polymer 2010, 51, 679.
5. Klein, R. J.; Runt, J. J Phys Chem B 2007, 111, 13188.
6. Shah, R. K.; Paul, D. R. Macromolecules 2006, 39, 3327.
7. Kulkarni, H. P.; Mogilevsky, G.; Mullins, W. M.; Wu, Y. J Mater Sci 2009, 24, 1087.

8. Lim, J. S.; Lee, Y.; Im, S. S. J Polym Sci Part B: Polym Phys 2008, 46, 925.
9. Atiqur, R. S.; Kitao, H.; Nemoto, N. Polymer 2004, 45, 4523.
10. Wu, Q.; Weiss, R. A. J Polym Sci Part B: Polym Phys 2004, 42, 3628.
11. Cooper, W. J Polym Sci 1958, 28, 195.
12. Sanjay, K.; Nayak, S. M. J Appl Polym Sci 2009, 112, 778.
13. Ghebremeskel, Y.; Weiss, R. A. J Polym Sci Part B: Polym Phys 2008, 46, 1602.
14. Wakabayashi, K.; Register, R. A. Polymer 2006, 47, 2874.
15. Luqman, M. Polymer 2008, 49, 1871.
16. Wang, W.; Chan, T.-T.; Perkowski, A.; Schlick, S.; Winey, K. I. Polymer 2009, 50, 1281.
17. Fitzgerald, J. J.; Weiss, R. A. J Polym Sci Part B: Polym Phys 1990, 28, 1719.
18. Kim, J. W.; Song, J. M.; Cho, Y. J.; Kim, J. S.; Yu, J. A. Polymer 2006, 47, 871.
19. Eisenberg, A.; Hird, B.; Moore, R. B. Macromolecules 1990, 23, 4098.
20. Benetatos, N. M.; Winey, K. I. J Polym Sci Part B: Polym Phys 2005, 43, 3549.
21. Makowski, H. S.; Lundberg, R. D.; Westerman, L.; Bock, J. Am Chem Soc Adv Chem Ser 1980, 187, 3.
22. Andreeva, E. D.; Nikitin, V. N.; Boyartchuk, Y. K. Macromolecules 1976, 9, 238.
23. Painter, P. C.; Coleman, M. M. Fundamentals of Polymer Science; Technomic: Lancaster, PA, 1994.
24. Coleman, M. M.; Lee, J. Y.; Painter, P. C. Macromolecules 1990, 23, 2339.
25. Kutsumizu, S.; Nagao, N.; Tadano, K.; Tachino, H.; Hirasawa, E.; Yano, S. Macromolecules 1992, 25, 6829.
26. (a) Gao, Y.; Choudhury, N. R.; Dutta, N.; Matisons, J.; Reading, M.; Delmotte, L. Chem Mater 2001, 13, 3644; (b) Capelle, H. A.; Britcher, L. G.; Morris, G. E. J Colloid Interface Sci 2003, 268, 293.
27. Young, S. K.; Trevino, S. F.; Tan, N. C. B. Polym Mater Sci Eng 2001, 85, 25.
28. Gao, Y.; Choudhury, N. R.; Dutta, N.; Shanks, R.; Weiss, B. J Therm Anal Cal 2003, 73, 361.
29. Duvdevani, I.; Lundberg, R. D.; Wood-Cordova, C.; Wilkes, G. L. Polym Prepr (Am Chem Soc Div Polym Chem) 1986, 184.
30. Jackson, D. A.; Weiss, R. A.; Koberstein, J. T. Polym Prepr (Am Chem Soc Div Polym Chem) 1991, 120.
31. Antony, P.; Bhattacharya, A. K.; De, S. K. J Appl Polym Sci 1999, 71, 1257.
32. Nishio, M.; Nishioka, A.; Taniguchi, T.; Koyama, K. Polymer 2005, 46, 261.
33. Xie, H. Q.; Ma, B. Y. J Macromol Sci Phys 1989, 28, 51.
34. Granick, S. J Appl Polym Sci 1983, 28, 1717.
35. TA Instruments: Newcastle, DE, 2003.
36. Wu, Q.; Weiss, R. A. Polymer 2007, 48, 7558.
37. Bonotto, S.; Bonner, E. F. Polym Prepr (Am Chem Soc Div Polym Chem) 1968, 537.
38. Kohzaki, M.; Tsujita, Y.; Takizawa, A.; Kinoshita, T. J Appl Polym Sci 1987, 33, 2393.